JOURNAL OF GEOPHYSICAL RESEARCH, VOL. 106, NO. C3, PAGES 4629–4638, MARCH 15, 2001

Field observations of wave-driven setdown and setup

B. Raubenheimer
Woods Hole Oceanographic Institution, Woods Hole, Massachusetts

R.T. Guza
Scripps Institution of Oceanography, La Jolla, California

Steve Elgar
Woods Hole Oceanographic Institution, Woods Hole, Massachusetts

Abstract. Wave-driven setdown and setup observed for 3 months on a cross-shore transect between the shoreline and 5 m water depth on a barred beach are compared with a theoretical balance between cross-shore gradients of the mean water level and the wave radiation stress. The observed setdown, the depression of the mean water level seaward of the surf zone, is predicted well when radiation stress gradients are estimated from the observations using linear theory at each location along the transect. The observed setdown also agrees with analytical predictions based on offshore wave observations and the assumption of linear, dissipationless, normally incident waves shoaling on alongshore homogeneous bathymetry. The observed setup, the superelevation of the mean water level owing to wave breaking, is predicted accurately in the outer and middle surf zone, but is increasingly underpredicted as the shoreline is approached. Similar to previous field studies, setup at a fixed cross-shore location increases with increasing offshore wave height and is sensitive to tidal fluctuations in the local water depth and to bathymetric changes. Numerical simulations and the observations suggest that setup near the shoreline depends on the bathymetry of the entire surf zone and increases with decreasing surf zone beach slope, defined as the ratio of the surf zone-averaged water depth to the surf zone width. A new empirical formula for shoreline setup on nonplanar beaches incorporates this dependence.

1. Introduction

Wave setdown and setup are changes in mean water level that accompany shoaling and breaking surface gravity waves. With no alongshore variations in waves or bathymetry and negligible wind and bottom stresses, the cross-shore pressure gradient associated with the time-averaged wave setdown and setup η theoretically balances the cross-shore gradient of the time- and depth-averaged onshore wave momentum flux (the wave radiation stress S_{xx}) [*Longuet-Higgins and Stewart,* 1962],

$$\frac{\partial S_{xx}}{\partial x} + \rho g(\eta + h)\frac{\partial \eta}{\partial x} = 0 \qquad (1)$$

where x is the cross-shore coordinate, h is the still water depth, ρ is the water density, g is gravitational acceleration, and for linear, shoreward propagating, monochromatic waves,

$$S_{xx} = E\left\{[\cos^2(\theta) + 1]\frac{C_g}{C} - \frac{1}{2}\right\}, \qquad (2)$$

where E is the wave energy, θ is the wave direction, and C_g and C are the group and phase velocities, respectively.

The theoretical balance (1), with S_{xx} given by (2), is consistent with observations in narrow wave flumes (where θ = 0) with smooth, impermeable, fixed bottoms and planar [*Bowen et al.,* 1968], barred [*Battjes and Janssen,* 1978; *Battjes and Stive,* 1985], and other [*Gourlay,* 1992] depth profiles. Predictions of setup differ in detail because of different model dependencies of S_{xx} on local wave properties (e.g., linear or nonlinear theory) and different formulations of the effect of wave rollers [e.g., *Svendsen,* 1984; *Diegaard et al.,* 1991; *Schäffer et al.,* 1993].

There are few field tests of the balance (1) using concurrent observations of both η and S_{xx} across the surf zone. *Battjes and Stive* [1985] integrated (1) using a wave transformation model to predict S_{xx} and obtained good agreement with setup observed in 2 and 4 m depth during a storm. Assuming that the depth and setup vary linearly across the beach, *Lentz and Raubenheimer* [1999] showed that the setup measured for 3.5 years in 2 m water depth was modeled qualitatively well by (1) with S_{xx} estimated with (2) using wave measurements in 8 and 2 m depths. However, the assumptions of linear depth and setup variations were shown to lead to integration errors as large as 50% of the observed setup. More accurate setup predictions with S_{xx}

Paper number 2000JC000572.
0148-0227/01/2000JC000572$09.00

and h estimated from wave and bathymetry data collected along a cross-shore transect agreed well with setup observed for 2 months in 2 m water depth, even though the setup measurements were made with unburied pressure sensors subject to flow-induced measurement errors (see Appendix A) and offset drift.

Field measurements show that surf zone setup depends on the local water depth and the offshore wave height [*Nielsen,* 1988; *King et al.,* 1990]. Field observations of setup at the shoreline η_{shore} suggest

$$\eta_{\text{shore}} = cH_{s,0}, \tag{3}$$

where $H_{s,0}$ is the offshore significant wave height and c is a constant between about 0.2 and 0.3 [*Hansen,* 1978; *Guza and Thornton,* 1981; *Nielsen,* 1988; *Hanslow et al.,* 1996]. This result is consistent with (1) and (2) assuming a monotonic beach slope, normally incident long waves, and surf zone wave heights that are a constant fraction of the water depth. However, scatter about (3) is considerable (often greater than 100% of η_{shore}), possibly because natural beaches often are barred or alongshore inhomogeneous, wave reflection may be large near the shoreline, and the ratio of wave height to water depth may depend on the beach slope and wave conditions. Additionally, observed mean water levels near the shoreline (in both field and laboratory studies) can be sensitive to the measurement technique [e.g., *Holland et al.,* 1995] and to the definition of setup [e.g., *Gourlay,* 1992].

In contrast to (3), *Holman and Sallenger* [1985] found no correlation between video-based estimates of η_{shore} and $H_{s,0}$, but instead suggested that $\eta_{\text{shore}}/H_{s,0}$ increased with increasing Iribarren number $\xi_0 = \beta/\sqrt{H_{s,0}/L_0}$, where β is the foreshore beach slope and L_0 is the offshore wavelength of the spectral peak frequency. Scatter in this relationship was reduced by separating the results into low, middle, and high tidal stages, and it was hypothesized that the offshore bar morphology influenced the low-tide shoreline setup. However, the observations of *Nielsen* [1988] showed little effect of the offshore barred bathymetry on the setup, and thus the importance of barred bathymetry to η_{shore} is uncertain.

Here the balance (1) is tested with field observations of waves and time-averaged water levels measured between the shoreline and about 5 m water depth on a barred beach. Water levels are estimated with buried, stable pressure sensors. Setdown and setup up are predicted by integrating (1) with S_{xx} based on (2) using the wave observations. The observed setdown is consistent with (1). Similar to *Lentz and Raubenheimer* [1999], setup is predicted well in 2 m water depth, but the balance breaks down in depths shallower than about 1 m. Setup near the shoreline is shown to be sensitive to the surf zone bathymetry and tidal fluctuations.

2. Field Experiment and Data Processing

Observations were acquired from September through November 1997 on a sandy Atlantic Ocean beach near Duck, North Carolina. Bottom pressure was measured with 12 buried pressure gages (setup sensors) located between the shoreline and about 5 m water depth (Figure 1, solid circles). The setup pressure sensors were buried to avoid flow-induced deviations from hydrostatic pressure (see Appendix A). After correcting for temporal changes in water density [*Lentz and Raubenheimer,* 1999] with conductivity and temperature measured in 5 m water depth, mean water levels were calculated from 512 s (8.5 min) records by assuming hydrostatic pressure.

Setup (setdown) was defined as the increase (decrease) of the mean water level relative to that observed at the most offshore setup sensor (cross-shore location $x = 58$ m). The observed shoreline setup was estimated as the setup where the total water depth was < 0.1 m. Note that η_{shore} was measured only when the shoreline, defined as the intersection of the mean water level with the beach, approximately coincided with a setup sensor location, which occurred at most once per rising (and falling) tide.

At all but the shallowest three locations, sensor offset drifts (typically equivalent to about 0.03 m of water over the 3 month experiment) were removed by subtracting from each time series a quadratic curve fit to setup estimated at 17 times when negligible setup or setdown was expected ($H_{s,0} < 0.35$ m and $h > 2$ m). In shallower water ($x > 350$ m), drifts were removed by adjusting the calculated mean water levels (using a quadratic fit) so that setup and setdown were negligible for small nonbreaking waves (estimated as locations and times when the ratio γ_s of significant wave height H_s to total water depth $h + \eta$ was < 0.2) and so that the water level equaled sand level when the saturated sand above swash zone sensors first was exposed during rundown [*Raubenheimer et al.,* 1995].

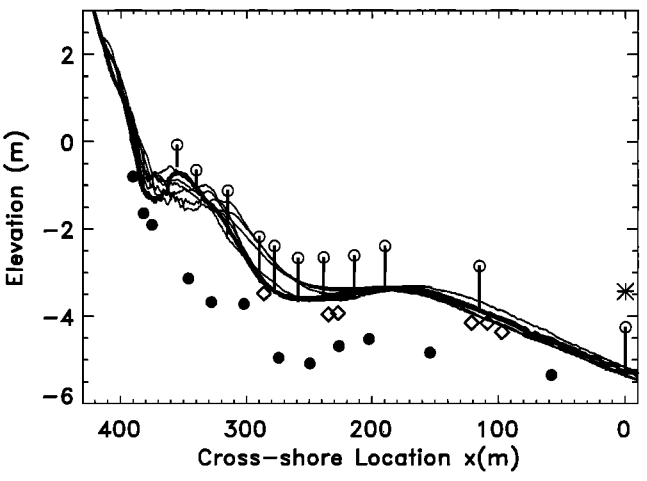

Figure 1. Locations of deeply buried pressure sensors used to measure setup (solid circles), colocated unburied pressure sensors, current meters, and sonar altimeters (open circles), near-bed pressure sensors (open diamonds), and the conductivity sensor (asterisk). The most seaward 11 setup sensors were accurate Paroscientific gages. All pressure measurements were corrected for temperature effects. The solid curves are selected beach profiles measured between 1 September and 31 November. The thick black curve is the 13 September profile. The x axis is positive onshore with the origin at the location of the offshore sensor.

Beach profiles were surveyed every few days with an amphibious vehicle, and seafloor elevations were measured nearly continuously at 11 cross-shore locations (Figure 1) with sonar altimeters [*Elgar et al.*, 2001]. Foreshore sand levels at the three shallowest setup gages (cross-shore locations 375, 382, and 390 m) were measured approximately daily using reference rods.

Significant wave heights (4 times the standard deviation of sea surface elevation fluctuations) and centroidal frequencies in the wind-wave frequency (f) band ($0.05 \leq f \leq 0.30$ Hz) were calculated every 512 s using observations from the three most shoreward setup sensors and from the wave sensors (Figure 1, open symbols) located between the setup sensors. Attenuation of pressure fluctuations through the water and the saturated sand above the buried setup sensors was accounted for using linear wave and poroelastic theories, respectively [*Raubenheimer et al.*, 1998]. Orbital velocities observed with bidirectional electromagnetic current meters were used to estimate 3 hour mean (energy-weighted average over frequency) wave directions [*Kuik et al.*, 1988, *Herbers et al.*, 1999]. Waves were assumed normally incident onshore of the shallowest current meter ($x > 350$ m).

Offshore (Figure 1, $x = 0$ m) wave heights (Figure 2a), directions, and centroidal frequencies ranged from 0.20 to 2.85 m, -35° to 35°, and 0.09 to 0.20 Hz, respectively. The maximum setup (0.547 m) was observed near the shoreline, and the maximum setdown (-0.033 m) was observed in 1.5-3.0 m water depth (Table 1).

Table 1. Least Squares Linear Fits (With Intercept a and Slope b) of Setup Predictions to Observations, and Range of Observed Setup for Different Total Depth ($h + \eta$) Ranges

Total Depth	$\eta_{pred} = a + b\eta_{obs}$			Range
m	a, m	b	correlation	η_{obs}, m
4.0 to 5.0	0.000	0.98	1.00	-0.016 to 0.112
3.0 to 4.0	0.000	0.98	1.00	-0.017 to 0.167
2.5 to 3.0	0.000	0.98	1.00	-0.033 to 0.171
2.0 to 2.5	0.001	0.95	0.99	-0.032 to 0.203
1.5 to 2.0	0.002	0.94	0.99	-0.033 to 0.236
1.0 to 1.5	0.002	0.93	0.99	-0.030 to 0.248
0.8 to 1.0	0.000	0.87	0.98	-0.022 to 0.269
0.6 to 0.8	0.005	0.69	0.97	-0.019 to 0.275
0.4 to 0.6	0.007	0.64	0.96	-0.025 to 0.304
0.2 to 0.4	0.009	0.57	0.92	-0.021 to 0.372
0.0 to 0.2	0.027	0.45	0.88	-0.013 to 0.547

3. Model Solutions

Cross-shore integration of (1) yields

$$\eta = -\int_{x_1}^{x_2} \frac{1}{\rho g(\eta + h)} \frac{\partial S_{xx}}{\partial x}\, dx, \qquad (4)$$

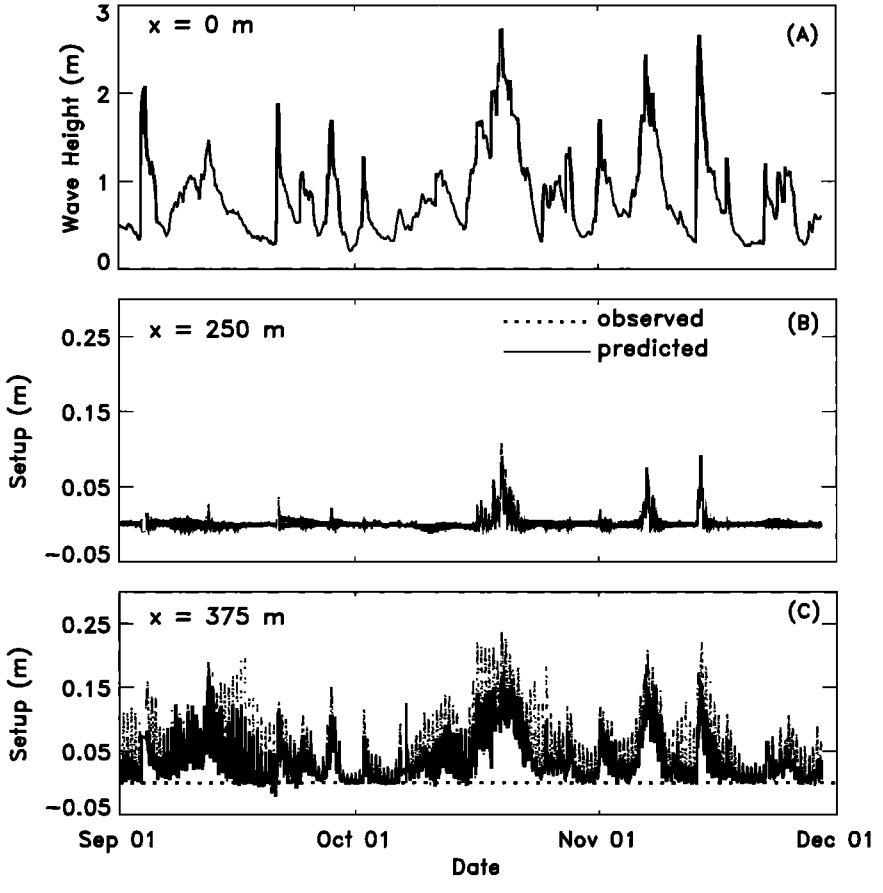

Figure 2. Observed (a) offshore ($x = 0$ m) significant wave height and observed (dotted curve) and predicted (solid curve) setup at cross-shore locations (b) $x = 250$ and (c) $x = 375$ m versus time. The horizontal dotted line in Figure 2c is the still water level (setup equal to 0.0 m).

where η is the sea level difference (i.e., the relative setdown or setup) between cross-shore locations x_1 and x_2. The integrated setup balance (4), with the wave radiation stress given by (2), is solved numerically for η relative to $x_1 = 58$ m using a fourth-order Runga-Kutta scheme with an adaptive step size for all 512 s data records. In (2) the wave energy is estimated as $E = \rho g H_s^2/16$; the wave direction θ is estimated as the mean direction; and the group and phase velocities C_g and C are estimated using linear theory, the centroidal frequency, and the total water depth $(h + \eta)$. Significant wave heights, mean wave directions, and centroidal frequencies are interpolated linearly between observation locations. The depth h, calculated from the most recent beach survey and the mean water level (relative to mean sea level) observed at the most offshore setup sensor ($x = 58$ m, Figure 1), includes tides and other processes (e.g., wind-driven setup) that affect the water level across the entire surf zone.

Setup contributes to the total water depth in (4) and also affects the group velocity and phase speed. Therefore (4) is solved iteratively by assuming that η at each shoreward step initially is equal to η at the neighboring offshore location.

Differences are small (0.00 ± 0.01 m) between hourly averaged setup based on S_{xx} calculated using the bulk wave properties (θ mean, H_s, C_g, and C described above) and hourly setup estimates based on wave radiation stresses estimated as $\int S_{xx}(f)df$, where $S_{xx}(f)$ is calculated with a directional moment technique [*Herbers and Guza,* 1990; *Elgar et al.,* 1994].

In 8-13 m water depth at this field site, mean water level changes driven by the cross-shore wind stress and by the Coriolis force associated with the alongshore flow can be comparable to wave-driven water level changes [*Lentz et al.,* 1999]. However for the conditions considered here, the estimated water level changes onshore of x_1 (depth about 5 m) owing to the wind stress and Coriolis force are at least an order of magnitude smaller than those caused by waves and therefore are neglected.

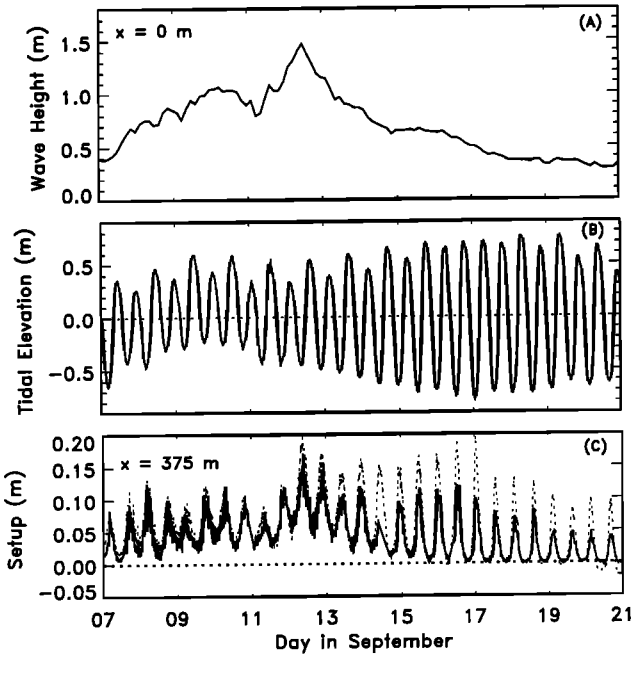

Figure 3. (a) Observed offshore ($x = 0$ m) wave heights, (b) observed offshore tidal elevation (8.5 min averaged sea surface level) (solid curve) relative to mean sea level (horizontal dotted line), and (c) observed (dotted curve) and predicted (solid curve) setup at cross-shore location $x = 375$ m versus time. The horizontal dotted line in Figure 3c is the still water level (setup equal to 0.0 m).

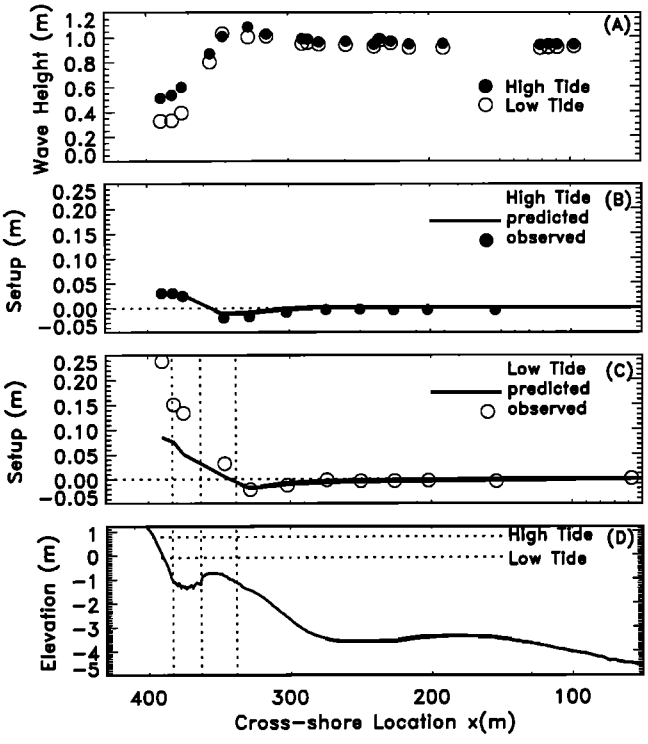

Figure 4. (a) Observed significant wave heights on 13 September, and observed (open circles) and predicted (solid curve) setdown and setup on 13 September at (b) high tide (1600) and (c) low tide (2042), and (d) measured beach profile versus cross-shore location (times represent the start of each 512 s record). The vertical dotted lines in Figures 4c and 4d mark the locations $x = 338$, 363, and 383 m discussed in the text. The horizontal dotted lines in Figures 4b and 4c are still water level. The horizontal dotted lines in Figure 4d are tidal elevations during the two runs.

4. Observations of Setup and Comparisons With Predictions

4.1. Observations

Consistent with empirical formulas [e.g., *Nielsen,* 1988; *Gourlay,* 1992] and previous observations, the setup observed at fixed locations increases with increasing offshore wave height $H_{s,0}$ (Figure 2). Near the shoreline ($x = 375$ m; Figures 2c and 3c) the measured setup also is sensitive to changes in the local depth owing to tides and bathymetric evolution. During each tidal cycle the setup observed at a fixed surf zone location is larger at lower tide when the observation location is closer to the shoreline (Figure 3c; and compare the three data points for $x \geq 375$m in Figure 4b with those in Figure 4c). With approximately equal

offshore wave heights, the setup observed at x = 390 m increases from 0.03 m at high tide to 0.23 m at low tide as the tidal elevation decreases by 0.9 m (Figure 4). Consistent with previous laboratory [*Bowen et al.*, 1968] and field [*Nielsen*, 1988] studies, the slope of the mean water level at the most shoreward setup observations is approximately twice as steep as that farther offshore (Figures 4 and 5a).

It has been suggested [*Nielsen*, 1988; *Hanslow et al.*, 1996] that cross-shore profiles of setup (normalized by the offshore wave height) can be parameterized as a function of the local water depth (normalized by the offshore wave height). However, on barred profiles the setup often is different at locations on the outer slope of the bar, in the trough of the bar, and on the foreshore even though the water depths are identical at the three locations (x = 338, 363, and 383 m in Figure 4c) where the depth is 1 m. The observed setup in the trough is consistently higher than that observed in similar depths offshore of the bar (Figure 5a; compare values at constant $h/H_{s,0}$).

4.2. Comparison With Predictions

Setdown and setup are predicted well (using (4) and (2)) except near the shoreline where setup is underpredicted (e.g., x = 375 m at low tide in Figures 2c and 3c). With moderate wave conditions, the heights of nonbreaking shoaling waves increase on the offshore slope of the sand bar (200 < x < 350 m, Figure 4a), and setdown is observed and predicted (Figures 4b and 4c). Farther onshore, breaking reduces the wave heights, and setup is observed and predicted. At low tide the setup on the foreshore is underpredicted (Figure 4c; and compare setup observations with setup predictions for the smallest normalized depths in Figure 5).

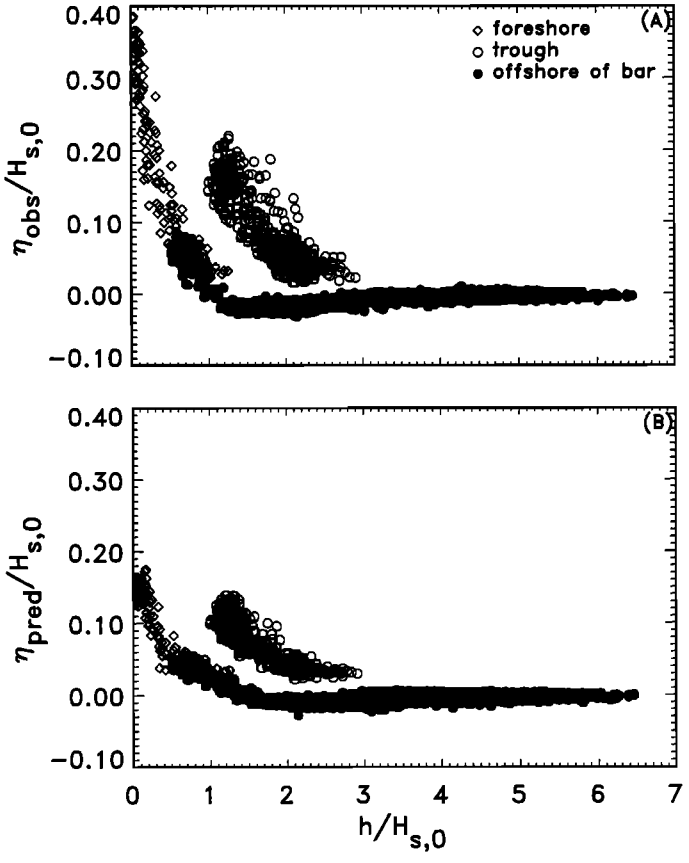

Figure 5. (a) Observed and (b) predicted normalized (by offshore wave height) setup versus normalized water depth for all 8.5 min runs between 13 September 0100 and 14 September 0100. Cross-shore locations are foreshore x > 383 m (diamonds), trough 383 ≤ x ≤ 363 m (open circles), and offshore of bar crest x < 363 m (solid circles). Offshore wave heights ranged from 0.75 to 1.00 m.

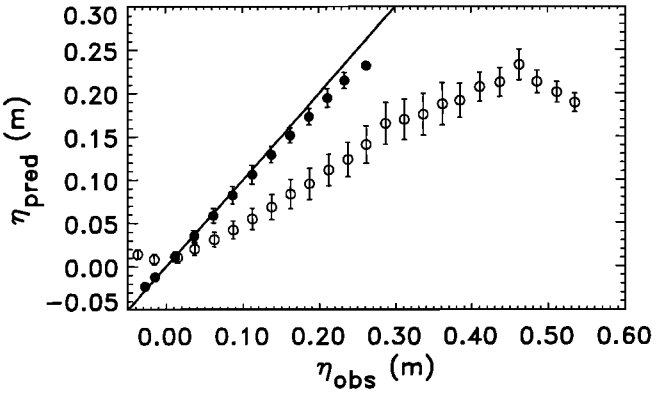

Figure 6. Predicted versus observed mean (circles) and standard deviation (vertical bars) of 512 s setdown and setup in total water depths of less than (open circles) and greater than (solid circles) 1 m.

Setup is predicted accurately in water depths > 1 m for the entire 3 month long data set (solid symbols in Figure 6), but setup is underpredicted in shallower water depths (open symbols in Figure 6). In all depths the least squares linear fits of the predictions to the observations have small intercepts relative to the range of setup values (Table 1). However, the regression slopes indicate increasing underprediction of setup in depths < 1 m, reaching a maximum underprediction of about a factor of 2 near the shoreline (Figure 7 and Table 1). The cause of the underpredictions is unknown. The correlation between the observations and predictions is > 0.88 in all water depths.

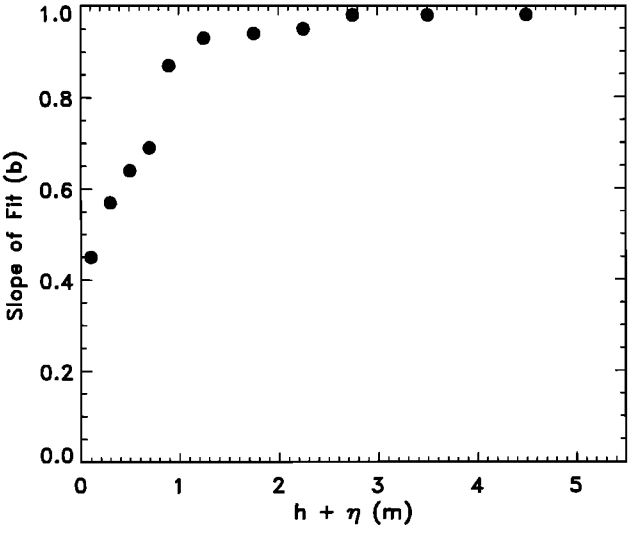

Figure 7. Slope of least squares fit of setup predictions to observations (b in Table 1) versus total water depth ($h + \eta$).

Setdown in the shoaling region is predicted well (root-mean-square (RMS) error 0.002 m) by the numerical model ((4) and (2) with S_{xx} estimated from observations along the transect) (Figure 8a). Assuming linear shoreward propagating, monochromatic, nondissipative waves, S_{xx} can be predicted analytically and the setdown is given by [*Longuet-Higgins and Stewart*, 1964]

$$\eta = -a_d^2 k_d f(k_d h), \tag{5}$$

where

$$f(k_d h) = -\frac{1}{2}\frac{\coth^2 kh}{2kh + \sinh 2kh}, \qquad k_d h = kh \tanh kh, \tag{6}$$

where a_d and k_d are the deep water wave amplitude and wavenumber, respectively. For narrow-banded (in frequency) random waves $a_d = H_{s,d}/(2\sqrt{2})$ and

$$\eta = -\frac{H_{s,d}^2 k_d}{8} f(k_d h) \tag{7}$$

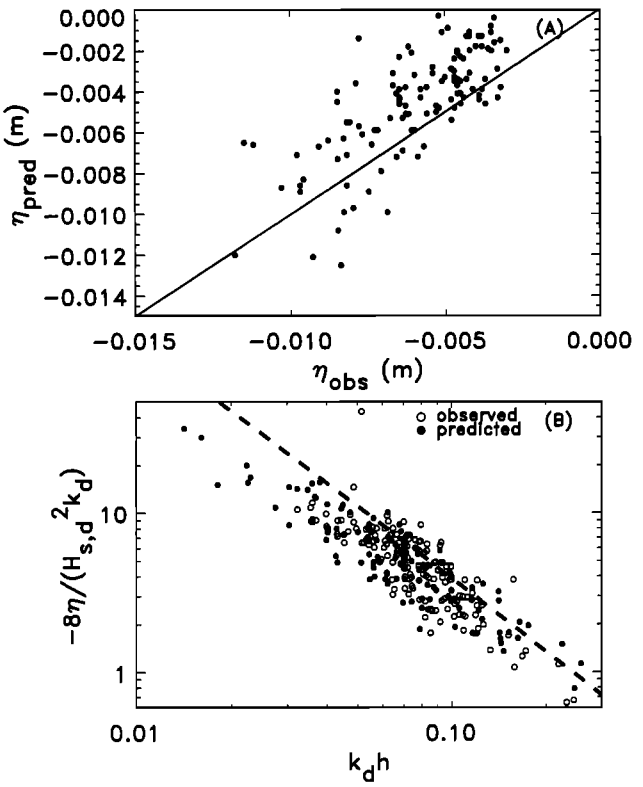

Figure 8. (a) Numerically predicted (with (4)) versus observed hourly averaged setdown for data where the observed setdown is larger than 0.003 m and (to avoid breaking waves) the observed γ_s is less than or equal to 0.2. The solid diagonal line is $\eta_{obs} = \eta_{pred}$. The correlation coefficient and RMS error between observations and predictions are 0.75 and 0.002 m, respectively. (b) Observed (open circles) and numerically predicted (solid circles) normalized (by deep water wave height squared $H_{s,d}^2$ and wavenumber k_d) hourly averaged setdown versus normalized local water depth. The dashed line is (7). The RMS errors between the analytical estimates (7) and the observed and numerically predicted η are 0.004 and 0.003 m, respectively.

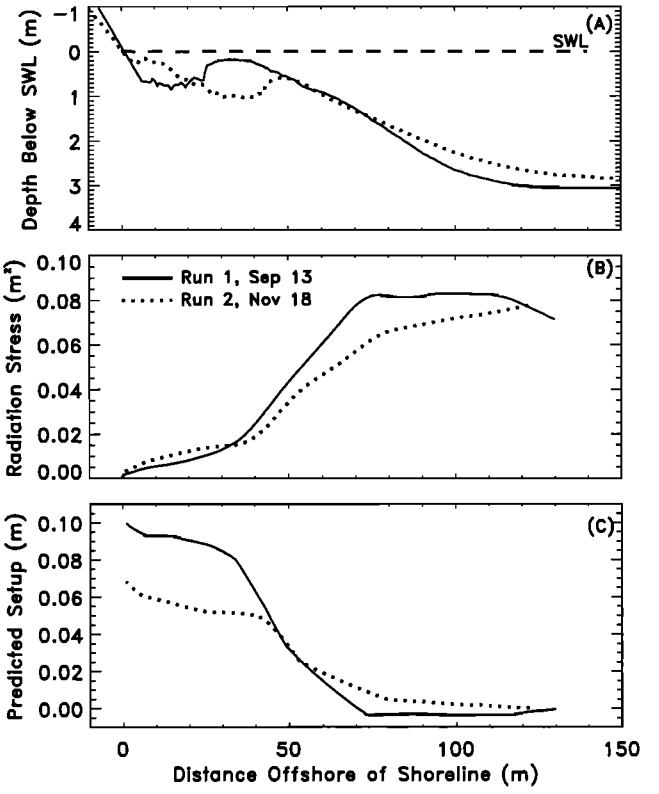

Figure 9. Model simulations show the effect of two bathymetries on setup. In both simulations, Rbreak is initialized with the pressure and velocity time series and tidal elevations observed on 13 September 2140-2148. (a) Observed depth profiles relative to still water level (SWL, the horizontal dashed line), (b) Rbreak-predicted wave radiation stress S_{xx}, and (c) simulated (using (4)) setdown and setup versus the distance offshore of the shoreline. The solid and dotted curves in Figures 9b and 9c are results for the 13 September 2140 (run 1) and 18 November 0450 (run 2) depth profiles (shown in Figure 9a), respectively.

where k_d is now the wavenumber of the spectral peak. The deep water values of $H_{s,d}$ and k_d are estimated using the observations at the offshore sensor ($H_{s,0}$ and k_0 at $x = 0$ m) and linear theory. Similar to laboratory observations [*Bowen et al.*, 1968], the observed (and predicted) setdown is modeled well by (7) (Figure 8b).

5. Discussion

5.1. Importance of Bathymetry and Tidal Elevation

The importance of bathymetry and tidal fluctuations to the wave-driven setup is investigated by driving the numerical setup model (4) with wave radiation stresses estimated using (2) and wave properties (H_s, C_g, and C) calculated from sea surface elevation fluctuations predicted by a numerical model (Rbreak) based on the nonlinear shallow water equations [*Kobayashi et al.*, 1989; *Raubenheimer et al.*, 1996]. To test the wave model, Rbreak is initialized at $x = 260$ m (water depth 3.23 m) with pressure and velocity time series measured on 13 September from 1917 until 2200. Wave radiation stresses calculated from Rbreak are within 6% of

those estimated from the observations (not shown).

To examine bathymetric effects, Rbreak model simulations are initialized with pressure and velocity time series (H_s = 0.8 m) and tidal level (−0.57 m) measured on 13 September 2140-2148 at cross-shore location x = 260 m (Figure 1), but are run on two different observed bathymetries (13 September (run 1) and 18 November (run 2)). For both runs the model is initialized in 3 m water depth, which occurs at distances 130 and 125 m offshore of the shoreline on the 13 September and 18 November bathymetries, respectively. In the inner surf zone (within about 50 m of the shoreline) the setup predicted using (4) and the Rbreak-simulated wave conditions is 25% larger on the run 1 bathymetry than on the run 2 bathymetry (Figure 9). For a given radiation stress decrease, the setup gradient (1) increases with decreasing water depth [e.g., *Battjes and Janssen,* 1978], so relatively large setup occurs on the shallow bar crest (offshore distance 30-50 m) of run 1. The effects of changes in tidal elevation are illustrated by comparing setup predicted using

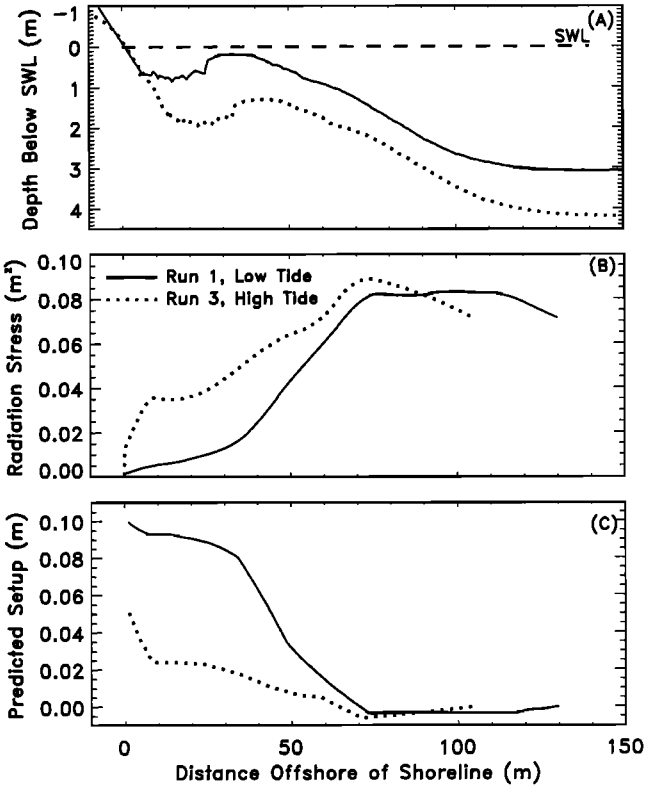

Figure 10. Model simulations show the effect of two tidal elevations on setup. In both simulations, Rbreak is initialized with the pressure and velocity time series and bathymetry observed on 13 September 2140-2148. (a) Observed depth profiles relative to still water level (SWL, the horizontal dashed line), (b) Rbreak-predicted wave radiation stress S_{xx}, and (c) simulated (using (4)) setdown and setup versus the distance offshore of the shoreline. The bar crest in Figure 10a is both deeper and farther from the shoreline at high tide than at low tide. The solid and dotted curves in Figures 10b and 10c are results for the 13 September 2140 (run 1, tidal level -0.57 m) and 13 September 1645 (run 3, tidal level +0.57 m) tidal elevations, respectively.

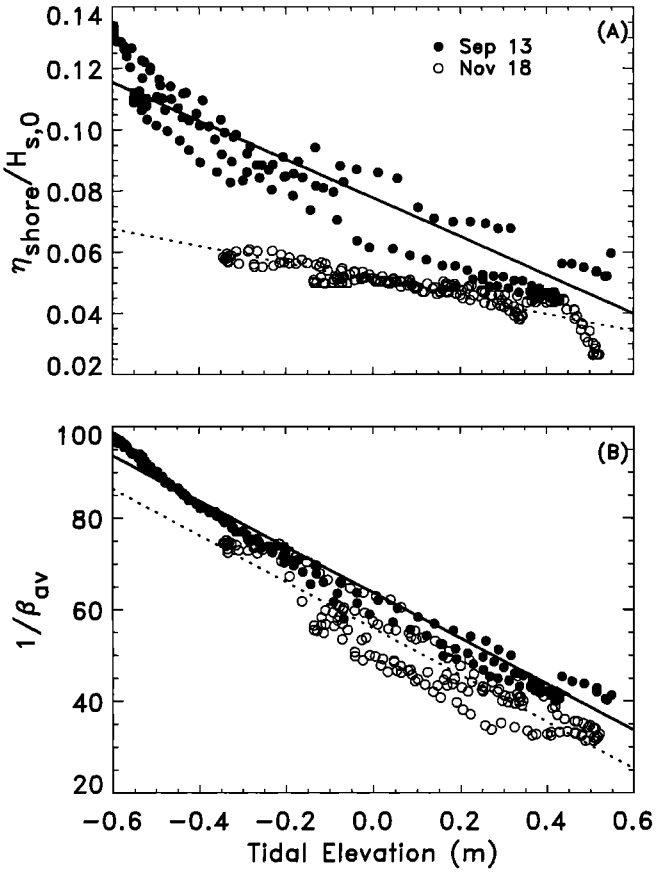

Figure 11. (a) Normalized (by offshore wave height) shoreline setup predictions (using (4)) driven with observed wave radiation stresses and (b) inverse of the surf zone-averaged beach slope (8) versus tidal elevation for all 512 s records on 13 September (solid circles) and 18 November (open circles). The least squares linear fits to the 13 September and 18 November predictions are shown by the solid and dotted lines, respectively. The range of offshore wave heights was 0.75-1.00 m on 13 September and 0.65-0.95 m on 18 November.

(4) and Rbreak wave properties simulated with the same incident wave conditions and the 13 September bathymetry, but with different tidal levels (−0.57 (run 1) and 0.57 m (run 3)). The model is initialized in 3 m water depth, which in these cases occurs at distances 130 and 105 m offshore of the shoreline for tidal levels −0.57 and 0.57 m, respectively. As shown in Figure 10, more setup is predicted at low tide when dissipation is strong over the shallow bar crest (run 1) than at high tide when the bar crest is in deeper water (run 3).

In all three runs the offshore wave conditions are identical, and the foreshore beach slopes are similar. The differences in modeled setup suggest that some of the scatter of observed η_{shore} about empirical formulas based on wave parameters offshore of the surf zone and foreshore beach slopes [e.g., *Holman and Sallenger,* 1985; *Nielsen,* 1988] may be caused by changing surf zone bathymetry and water levels.

The effects of bathymetry and tidal fluctuations also are apparent in the shoreline setup (Figure 11) predicted by the numerical setup model (4) driven with the observed waves

and bathymetry for 24 hours (170 512-s runs) on both 13 September and 18 November. Wave conditions and tidal ranges were similar during the 2 days, but the bathymetries differed substantially (Figure 9a). The predicted shoreline setup (normalized by the offshore wave height) is larger on 13 September than on 18 November for almost all tidal elevations (Figure 11a). Furthermore, in contrast to (3) in which $\eta_{\text{shore}}/H_{s,0}$ is constant, on both profiles the normalized shoreline setup increases with decreasing tidal elevation. On a planar beach, tidal fluctuations do not affect the average surf zone beach slope β_{av}:

$$\beta_{av} = \frac{h_{av}}{\Delta x}, \tag{8}$$

where

$$h_{av} = \frac{1}{\Delta x}\int (h+\eta)dx, \tag{9}$$

with Δx the distance from the shoreline to the outer edge of the surf zone, defined as the most offshore location where $\gamma_s \geq 0.45$ [*Lentz and Raubenheimer*, 1999]. However, on the bathymetry considered here, β_{av} decreases with decreasing tidal elevation (Figure 11b). Although the shoreline setup (Figures 9, 10, and 11) is underpredicted by the numerical model (Figures 6 and 7), these results and those of *Hansen* [1978] suggest that the shoreline setup is sensitive to the surf zone water depth and surf zone width and may be correlated with β_{av}.

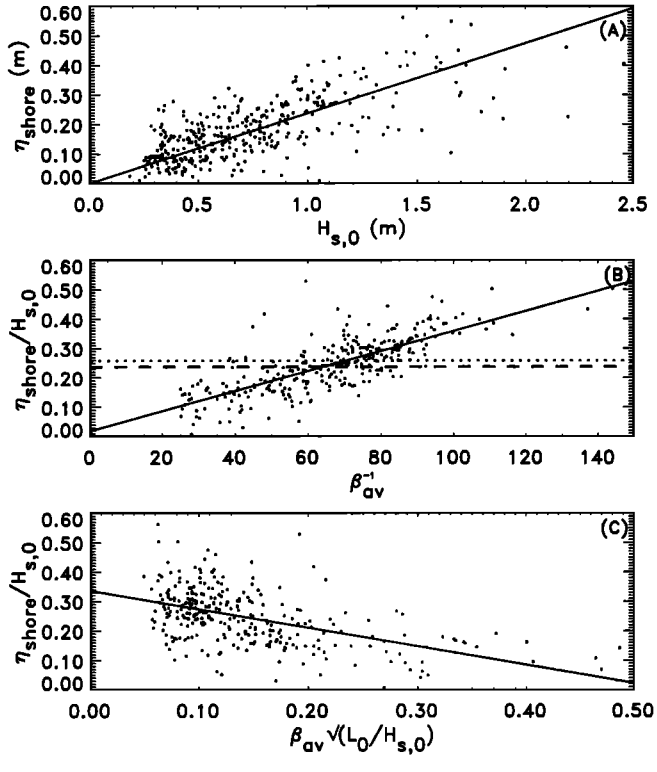

Figure 12. (a) Observed shoreline setup versus offshore significant wave height and (b) and (c) observed shoreline setup normalized by offshore significant wave height versus β_{av}^{-1} and $\beta_{av}\sqrt{L_0/H_{s,0}}$, respectively. The solid line in Figure 12a and the horizontal dashed line in Figure 12b are the least squares fit to (3) ($\eta_{\text{shore}} = cH_{s,0}$ where $c = 0.24$ and RMS error $= 0.10$). The horizontal dotted line in Figure 12b is the average normalized setup $(\eta_{\text{shore}}/H_{s,0})_{\text{avg}} = 0.26$, RMS error 0.10. The solid lines in Figures 12b and 12c are the least squares linear fits given by $\eta_{\text{shore}}/H_{s,0} = 0.019 + 0.003\beta_{av}^{-1}$, RMS error 0.06 (Figure 12b), $\eta_{\text{shore}}/H_{s,0} = 0.336 - 0.628\beta_{av}\sqrt{L_0/H_{s,0}}$, RMS error 0.08 (Figure 12c). RMS differences of 0.02 are statistically significant at the 98% level.

5.2. Empirical Formulas for Shoreline Setup

Consistent with previous observations and empirical formulas (e.g., (3)), the observed shoreline setup η_{shore} increases with increasing offshore wave height $H_{s,0}$ (Figure 12a). However, scatter about the least squares linear fit ($\eta_{\text{shore}}/H_{s,0} = 0.24$) is substantial (RMS error 0.10; Figure 12b). Better predictions of $\eta_{\text{shore}}/H_{s,0}$ result from a least squares linear fit to β_{av}^{-1} (RMS error 0.06; Figure 12b) or to a surf zone Iribarren number $\beta_{av}\sqrt{L_0/H_{s,0}}$ (RMS error 0.08; Figure 12c). In contrast to some previous observations, the correlation of $\eta_{\text{shore}}/H_{s,0}$ with Iribarren number where β is equal to the foreshore slope is not statistically significant (not shown). The best fit (RMS error 0.06) to the present observations on a barred beach ($0.01 \leq \beta_{av} \leq 0.04$) is given by

$$\eta_{\text{shore}}/H_{s,0} = 0.019 + 0.003\beta_{av}^{-1}. \tag{10}$$

6. Conclusions

Setup and setdown observed for 3 months between the shoreline and 5 m water depth on a barred beach were compared with model predictions based on a balance (1) between cross-shore gradients of mean water level and the wave radiation stress. The observed wave setdown is consistent with the observed radiation stress gradients (estimated using wave observations and (2)) and also with radiation stress gradients predicted analytically (7) using offshore wave observations and assuming normally incident, monochromatic, nondissipative waves (Figure 8). The observed wave setup is consistent with the radiation stresses estimated from observations in the outer and middle surf zone, but is underpredicted by roughly a factor of 2 in depths shallower than $\sim$ 1 m (Figures 2, 3, 4, 6, and 7). Similar to previous field studies, setup at a fixed cross-shore location increases with increasing offshore wave height and is sensitive to tidal fluctuations in the local water depth and to the local bathymetry (Figures 2, 3, and 4). Consistent with numerical simulations that suggest setup near the shoreline depends on the bathymetry of the entire surf zone (Figures 9, 10, and 11), the observed shoreline setup increases as the surf zone-averaged beach slope decreases (Figure 12b). A new empirical formula (10) for shoreline setup incorporates this dependence.

Appendix A: Flow Noise

Errors in the measured mean water level caused by flow around the unburied pressure sensors are investigated by comparing mean water levels estimated using deeply buried sensors with those estimated using unburied pressure sensors. Pressure sensors were housed in $\sim$ 8 cm diameter, 30 cm long cylinders that were oriented vertically with the pressure ports pointing upward. From Bernouilli's equation, dif-

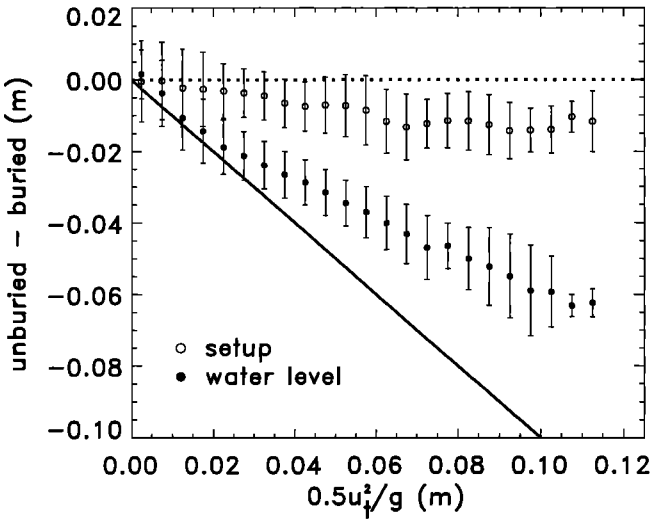

Figure A1. Mean (symbols) and standard deviations (vertical bars) of differences in mean water level (solid circles) and setup (open circles) estimated from measurements with buried and unburied pressure gages versus $0.5u_t^2/g$. Mean water level differences are calculated at all sensor locations. The solid line is a mean water level decrease equal to $0.5u_t^2/g$, a rough estimate of the dynamic pressure. Setup differences are estimated using measurements from all sensors located at $x > 214$ m relative to mean water levels estimated at $x = 214$ m and u_t (in the abscissa) measured at the shallower sensor location.

ferences in mean water level measured with colocated buried and unburied sensors are expected to be proportional to $0.5u_t^2/g$, where the total velocity $u_t = \sqrt{\tilde{u}^2 + \tilde{v}^2 + \bar{u}^2 + \bar{v}^2}$, with $\tilde{u}$, $\tilde{v}$, $\bar{u}$, and $\bar{v}$ the cross- and alongshore oscillatory and mean velocities, respectively. The constant of proportionality is ~ 1, but depends on the details of the flow around the unburied pressure sensors. Vertical velocities were not measured and are assumed small.

Most buried and unburied gages were not colocated (Figure 1). Therefore mean water levels estimated with buried gages are interpolated linearly to the locations of the unburied sensors. Mean levels measured near the water surface are noisy, perhaps owing to vertical flows, and thus observations from unburied sensors located $< 1.75H_s$ below the mean surface are excluded from the analysis. Differences in mean water level measured with buried and unburied pressure gages are roughly half $0.5u_t^2/g$ (Figure A1, solid circles).

Errors in mean water level estimated with unburied sensors are as large as 7 cm. However, owing to cancellation of flow-induced errors, setup estimated as the difference between mean water levels measured by two unburied sensors is within 2 cm of setup estimated as the difference between mean water levels measured by two buried sensors (Figure A1, open circles). Error cancellation is most complete between pairs of sensors located close to each other and thus in similar flow fields (not shown). These results support the speculation of *Lentz and Raubenheimer* [1999] that error cancellation contributed to the relatively good results obtained using unburied pressure sensors.

Acknowledgments. This research was supported by NSF and ONR. Staff from the Center for Coastal Studies deployed and maintained the instruments. The staff of the Field Research Facility assisted with the instrument deployment and provided the bathymetric surveys. Woods Hole Oceanographic Institution contribution 10240.

References

Battjes, J. A., and J. P. F. M. Janssen, Energy loss and setup due to breaking of random waves, paper presented at 16th International Conference on Coastal Engineering, ASCE, Hamburg, Germany, 1978.

Battjes, J. A., and M. J. F. Stive, Calibration and verification of a dissipation model for random breaking waves, *J. Geophys. Res., 90,* 9159-9167, 1985.

Bowen, A. J., D. L. Inman, and V. P. Simmons, Wave 'setdown' and wave setup, *J. Geophys. Res., 73,* 2569-2577, 1968.

Diegaard, R., P. Justesen, and J. Fredsøe, Modeling of undertow by a one-equation turbulence model, *Coastal Eng., 15,* 431-458, 1991.

Elgar, S., T. H. C. Herbers, and R. T. Guza, Reflection of ocean surface gravity waves from a natural beach, *J. Phys. Oceanogr., 24,* 1503-1522, 1994.

Elgar, S., R. T. Guza, W. C. O'Reilly, B. Raubenheimer, and T. H. C. Herbers, Wave energy and direction observed near a pier, *J. Waterw. Port Coastal Ocean Eng.,127,* 2-6, 2001.

Gourlay, M. R., Wave set-up, wave run-up, and beach water table: Interaction between surf zone hydraulics and groundwater hydraulics, *Coastal Eng., 17,* 93-144, 1992.

Guza, R. T., and E. B. Thornton, Wave setup on a natural beach, *J. Geophys. Res., 86,* 4133-4137, 1981.

Hansen, U. A., Wave setup and design water level, *J. Waterw. Port Coastal Ocean Div., 104,* 227-240, 1978.

Hanslow, D. J., P. Nielsen, K. Hibbert, Wave setup at river entrances, paper presented at 25th International Conference on Coastal Engineering, ASCE, Orlando, Fl., 1996.

Herbers, T. H. C., and Guza, R. T., Estimation of directional wave spectra from multi-component observations, *J. Phys. Oceanogr., 20,* 1703-1724, 1990.

Herbers, T. H. C., S. Elgar, and R. T. Guza, Directional spreading of waves in the nearshore, *J. Geophys Res., 104,* 7683-7693, 1999.

Holland, K. T., B. Raubenheimer, R. T. Guza, and R. A. Holman. Runup kinematics on a natural beach, *J. Geophys. Res., 100,* 4985-4993, 1995.

Holman, R. A., and A. H. Sallenger, Setup and swash on a natural beach, *J. Geophys. Res., 90,* 945-953, 1985.

King, B. A., M. W. L. Blackley, A. P. Carr, and P. J. Hardcastle, Observations of wave-induced setup on a natural beach, *J. Geophys. Res., 95,* 22,289-22,297, 1990.

Kobayashi, N., G. S. DeSilva, and K. D. Watson, Wave transformation and swash oscillation on gentle and steep slopes, *J. Geophys. Res., 94,* 951-966, 1989.

Kuik, A. J., G. P. van Vledder, and L. H. Holthuijsen, A method for routine analysis of pitch-and-roll buoy data, *J. Phys. Oceanogr., 18,* 1020-1034, 1988.

Lentz, S., and B. Raubenheimer, Field observations of wave setup dynamics, *J. Geophys. Res., 104,* 25,867-25,875, 1999.

Lentz, S., R. T. Guza, S. Elgar, F. Feddersen, and T. H. C. Herbers, Momentum balances on the North Carolina inner shelf, *J. Geophys. Res., 104,* 18,205-18,226, 1999.

Longuet-Higgins, M. S., and R. W. Stewart, Radiation stress and mass transport in gravity waves, with application to 'surf-beats,' *J. Fluid Mech., 13,* 481-504, 1962.

Longuet-Higgins, M. S., and R. W. Stewart, Radiation stresses in water waves: A physical discussion with applications, *Deep Sea Res., 11,* 529-562, 1964.

Nielsen, P., Wave setup: A field study, *J. Geophys. Res., 93,* 15,643-15,652, 1988.

Raubenheimer, B., R. T. Guza, S. Elgar, and N. Kobayashi, Swash

on a gently sloping beach, *J. Geophys. Res., 100,* 8751-8760, 1995.

Raubenheimer, B., R. T. Guza, and S. Elgar, Wave transformation across the inner surf zone, *J. Geophys. Res., 101,* 25,589-25,598, 1996.

Raubenheimer, B., S. Elgar, and R. T. Guza, Estimating wave heights from pressure measured in a sand bed, *J. Waterw. Port Coastal Ocean Eng., 124,* 151-154, 1998.

Schäffer, H. A., P. A. Madsen, and R. Deigaard, A Boussinesq model for waves breaking in shallow water, *Coastal Eng., 20,* 185-202, 1993.

Svendsen, I. A., Wave heights and setup in the surf zone, *Coastal Eng., 8,* 303-329, 1984.

S. Elgar and B. Raubenheimer, Woods Hole Oceanographic Institution, Woods Hole, MA 02543. (elgar@whoi.edu; britt@whoi.edu)

R. T. Guza, Scripps Institution of Oceanography, La Jolla, CA 92093. (rtg@coast.ucsd.edu)

(Received July 27, 2000; revised November 3, 2000; accepted November 27, 2000.)